Nonreciprocal Remanence Ferrite Phase Shifters Using the Grooved Waveguide

AKIHITO MIZOBUCHI AND HIDETOSHI KUREBAYASHI

Abstract—**For the purpose of improving the performance characteristics of the nonreciprocal remanence ferrite phase shifter, a new configuration with a grooved waveguide is proposed and analyzed. Some results calculated as functions of dielectric and ferrite thickness, waveguide dimensions, and frequency are shown and compared as being in good agreement with experiments at the *X* band. The figure of merit (differential phase shift per insertion loss) and the handling power of the proposed phase shifter are discussed in comparison with those of the conventional waveguide geometry.**

I. Introduction

THE NONRECIPROCAL remanence ferrite phase shifter has been used extensively as a beam-steering element in phased array radars because of its desirable characteristics [1]. Therefore, many techniques for improving the characteristics have been developed. For example, in order to optimize the figure of merit, Ince and Stern [2] have analyzed the phase shifter with a dielectric rib inserted into the slot of a ferrite toroid and obtained the optimum dimensions. Clark [3] also has investigated these devices with a chamfered ferrite toroid and succeeded in increasing the figure of merit by about 20 percent.

In order to realize high average-power capability, Whicker [4] and Rodrigue [5] adopted the configuration of a temperature-compensated garnet fabricated into a thin-walled toroid used with dielectric materials having high thermal conductivity. On the other hand, high peak-power capability is accomplished by increasing the spinwave linewidth ΔH_k or by decreasing the saturation magnetization $4\pi Ms$ of the material and also by adjusting the geometry of the device to reduce the maximum intensity of the RF magnetic field in the ferrite.

Up to this time, there have not been any techniques reported for improving the figure of merit and handling capabilities of both average and peak power, simultaneously.

In order to improve all of the characteristics mentioned above, we proposed a new configuration [6] of the nonreciprocal remanence ferrite phase shifter with a grooved waveguide. The advantages of the adoption of a grooved waveguide are as follows.

1) The figure of merit can be increased as a result of exciting a larger component of circular polarization within the ferrite.

2) An average power handling ability can be increased by reducing the thermal resistance between the ferrite and the waveguide.

3) The peak power handling capability is increased because the maximum RF magnetic field in the ferrite is reduced.

This paper describes the theoretical considerations and the experimental results of the phase shifter with the grooved-waveguide configuration.

II. Configuration

Two examples of new configurations are illustrated in Fig. 1, which consist of a ferrite toroid placed in the center of a grooved waveguide, a dielectric rib inserted into the slot of the ferrite, and a switching wire. In the configuration No. 2, the metal plates are placed so as to touch the center of the vertical ferrite walls.

III. Analysis

Fig. 2 shows the theoretical model and the coordinate system used in the analysis. With the assumption that the transverse electric field of the fundamental mode is parallel to the Z axis, the characteristic equation for computation of the normalized waveguide wavelength $(\lambda/\lambda g)$ can be obtained [2] as

$$\frac{\tan\left\{\frac{\Gamma_2\lambda_0}{2}\left(\frac{W_2}{\lambda_0}-\frac{W_1}{\lambda_0}\right)\right\}}{\Gamma_2\lambda_0}$$

$$=\Bigg[\frac{B}{G}(\Gamma_3\lambda_0)\cdot\cot\left\{\frac{\Gamma_3\lambda_0}{2}\left(\frac{W_3}{\lambda_0}-\frac{W_2}{\lambda_0}\right)\right\}-(\Gamma_1\lambda_0)\tan\left(\frac{\Gamma_1\lambda_0}{2}\cdot\frac{W_1}{\lambda_0}\right)\Bigg]\Bigg/\Bigg[\frac{1}{\mu_e}\cdot\left\{(\Gamma_2\lambda_0)^2+\left(2\pi\frac{K}{u}\cdot\frac{\lambda}{\lambda_g}\cdot\frac{F}{F_0}\right)^2\right\}$$

$$+\mu_e\frac{B}{G}(\Gamma_3\lambda_0)\cot\left\{\frac{\Gamma_3\lambda_0}{2}\left(\frac{W_3}{\lambda_0}-\frac{W_2}{\lambda_0}\right)\right\}\cdot(\Gamma_1\lambda_0)\tan\left(\frac{\Gamma_1\lambda_0}{2}\cdot\frac{W_1}{\lambda_0}\right)$$

$$+2\pi\frac{K}{u}\frac{\lambda}{\lambda_g}\frac{F}{F_0}\left(\frac{B}{G}(\Gamma_3\lambda_0)\cot\left\{\frac{\Gamma_3\lambda_0}{2}\left(\frac{W_3}{\lambda_0}-\frac{W_2}{\lambda_0}\right)\right\}+(\Gamma_1\lambda_0)\tan\left(\frac{\Gamma_1\lambda_0}{2}\cdot\frac{W_1}{\lambda_0}\right)\right)\Bigg] \quad (1)$$

Manuscript received May 24, 1978; revised August 4, 1978.
The authors are with the Mitsubishi Electric Corporation, 325 Kamimachiya, Kamakura City, Kanagawa, Japan 247.

0018-9480/78/1200-1012$00.75

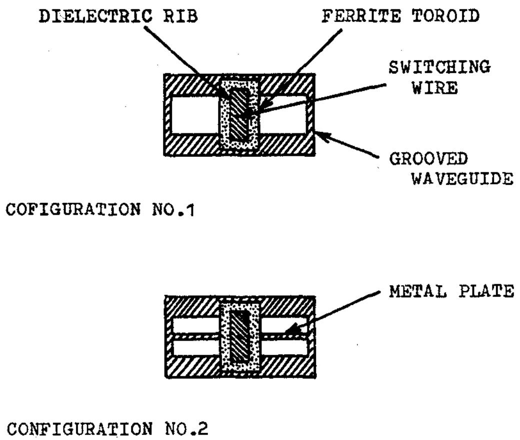

Fig. 1. New configuration of the nonreciprocal remanence ferrite phase shifter.

where

$$\Gamma_1\lambda_0=2\pi\frac{\lambda_0}{\lambda}\cdot\sqrt{\epsilon_1-\left(\frac{\lambda}{\lambda_g}\right)^2}\quad \Gamma_2\lambda_0=2\pi\frac{\lambda_0}{\lambda}\cdot\sqrt{\epsilon_2\mu_e-\left(\frac{\lambda}{\lambda_g}\right)^2}$$

$$\Gamma_3\lambda_0=2\pi\frac{\lambda_0}{\lambda}\cdot\sqrt{1-\left(\frac{\lambda}{\lambda_g}\right)^2}\qquad \mu_e=\frac{(\mu^2-K^2)}{\mu}$$

where μ and K are the diagonal and off-diagonal elements of the tensor permeability, and ϵ_1 and ϵ_2 are the permittivities of the dielectric and the ferrite, respectively. λ_0 is the free-space wavelength at the center frequency F_0. λ/λ_0 and λ_g/λ_0 are the normalized free-space and waveguide wavelength. F/F_0 is the normalized frequency.

The differential phase shift per unit length $\Delta\phi$ is

$$\Delta\phi=12\cdot\frac{\lambda}{\lambda_0}\cdot\left(\frac{\lambda_0}{\lambda_{g+}}-\frac{\lambda_0}{\lambda_{g-}}\right)\times 10^2\ \frac{\text{deg}}{\text{m}}\cdot\text{GHz} \tag{2}$$

where λ_{g+}/λ_0 and λ_{g-}/λ_0 are the solutions of (1) in the case of the positive and negative values of K corresponding to the positive and negative circular polarizations.

Various dimensions of the phase shifter, i.e., ferrite width, dielectric width, and grooved-waveguide width and height, should be determined so that only the fundamental mode propagates. The cutoff condition for the first higher order mode is computed by using the next higher root of the transcendental equation.

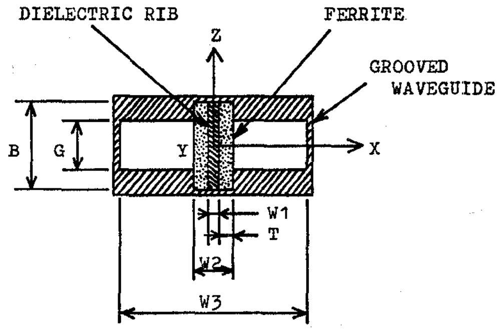

Fig. 2. Theoretical model of the nonreciprocal remanence ferrite phase shifter.

where

$$\Gamma_1'\lambda_0=2\pi\frac{\lambda_0}{\lambda}\sqrt{\epsilon_1}\qquad \Gamma_2'\lambda_0=2\pi\frac{\lambda_0}{\lambda}\sqrt{\epsilon_2\mu_e}$$

$$\Gamma_3'\lambda_0=2\pi\frac{\lambda_0}{\lambda}.$$

Furthermore, the losses can be obtained as the sum of dielectric, magnetic, and conductive loss components as follows:

$$\partial=\partial_d+\partial_m+\partial_c \tag{4}$$

$$\partial_d=\frac{\omega\epsilon_0\int_{\Delta S_1}\vec{E}\cdot\epsilon_1''\vec{E}^*\,dS+\omega\epsilon_0\int_{\Delta S_2}\vec{E}\cdot\epsilon_2''\vec{E}^*\,dS}{2\int_S\vec{i}y\cdot\frac{1}{2}(\vec{E}\times\vec{H}^*)\,dS}$$

$$\partial_m=\frac{\omega\mu_0\int_{\Delta S_2}\vec{H}^*\cdot\mu''\vec{H}\,dS}{2\int_S\vec{i}y\cdot\frac{1}{2}(\vec{E}\times\vec{H}^*)\,dS}$$

$$\partial_c=\frac{R_s\int_l|H_{\tan}|^2\,dl}{2\int_S\vec{i}y\cdot\frac{1}{2}(\vec{E}\times\vec{H}^*)\,dS}$$

where ω is the angular frequency, ϵ_1'' and ϵ_2'' are the imaginary parts of the permittivity of the dielectric and the ferrite, μ'' is the imaginary part of the permeability of the ferrite, R_s is the surface resistivity, and $\vec{i}_y$ is the unit vector in the y direction.

$$\frac{G}{B}\cdot\frac{\tan\left\{\frac{\Gamma_3'\lambda_0}{2}\cdot\left(\frac{W_2}{\lambda_0}-\frac{W_1}{\lambda_0}\right)\right\}}{\Gamma_3'\lambda_0}=-\frac{\left[\mu_e\dfrac{\Gamma_1'\lambda_0}{\tan\left(\frac{\Gamma_1'\lambda_0}{2}\frac{W_1}{\lambda_0}\right)}\cdot\dfrac{\tan\left\{\frac{\Gamma_2'\lambda_0}{2}\left(\frac{W_2}{\lambda_0}-\frac{W_1}{\lambda_0}\right)\right\}}{\Gamma_2'\lambda_0}+1.0\right]}{\left[\dfrac{\Gamma_1'\lambda_0}{\tan\left(\frac{\Gamma_1'\lambda_0}{2}\frac{W_1}{\lambda_0}\right)}-\dfrac{1}{\mu_e}(\Gamma_2'\lambda_0)\tan\left\{\frac{\Gamma_2'\lambda_0}{2}\left(\frac{W_2}{\lambda_0}-\frac{W_1}{\lambda_0}\right)\right\}\right]} \tag{3}$$

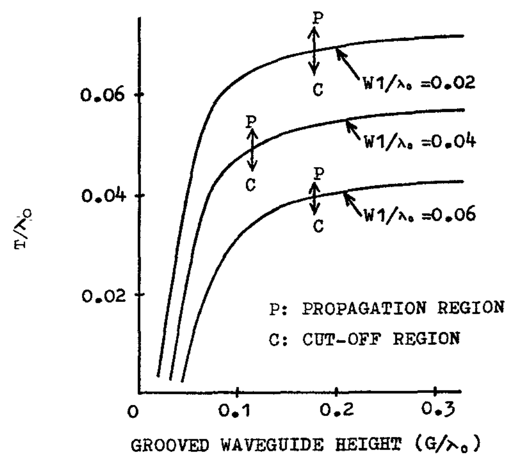

Fig. 3. Cutoff conditions for the first higher mode.

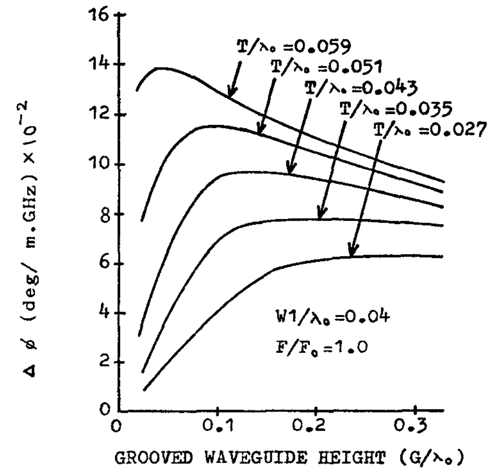

Fig. 5. Differential phase shift ($\Delta\phi$) versus grooved-waveguide height (G/λ_0) for several ferrite thicknesses (T/λ_0).

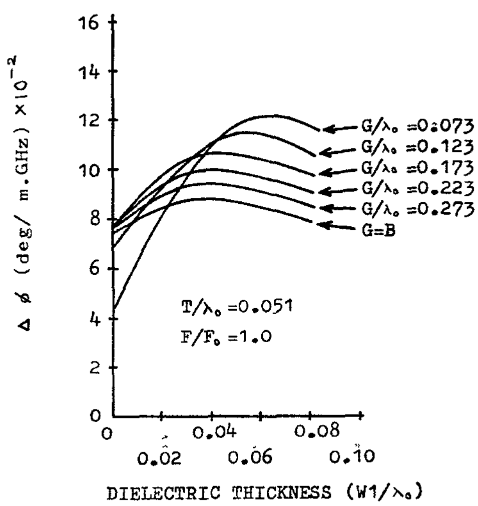

Fig. 4. Differential phase shift ($\Delta\phi$) versus dielectric rib thickness ($W1/\lambda_0$) for several grooved-waveguide heights (G/λ_0).

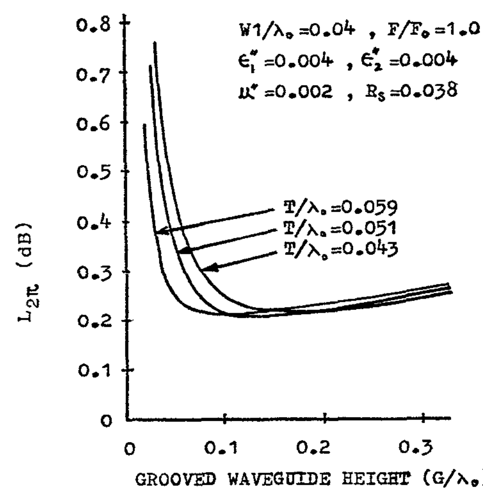

Fig. 6. Loss ($L_{2\pi}$) versus grooved waveguide height (G/λ_0) for several ferrite thicknesses (T/λ_0).

IV. Theoretical Characteristics

Theoretical characteristics are computed under the following conditions:

$$\epsilon_1 = 13.0 \quad \epsilon_2 = 12.0$$

$$\omega_m / F_0 = 0.67 \quad 4\pi Mr / 4\pi Ms = 0.774$$

$$B/\lambda_0 = 0.323 \quad W_3/\lambda_0 = 0.724$$

where γ is the gyromagnetic ratio, ω_m equals $\gamma \cdot 4\pi Ms$, and $4\pi Mr$ and $4\pi Ms$ are the remanent and saturation magnetization, respectively.

First of all, the calculation of the cutoff conditions for the first higher order mode is carried out by using (3), and the results are shown in Fig. 3, which reveals that, for example, ferrite thickness (T/λ_0) should be smaller than 0.055 when the grooved-waveguide height (G/λ_0) and dielectric rib thickness ($W1/\lambda_0$) are 0.2 and 0.04, respectively.

The influence of $W1/\lambda_0$ on the differential phase shift ($\Delta\phi$) is illustrated in Fig. 4. This figure shows that $\Delta\phi$ varies as a function of G/λ_0 and that there exists an optimum thickness of $W1/\lambda_0$ over the range from 0.03 to 0.06.

The variation of $\Delta\phi$ and $L_{2\pi}$ (loss per 360° of differential phase shift) with G/λ_0 for several values of T/λ_0 is shown in Figs. 5 and 6, which show that an increase in $\Delta\phi$ and, consequently, a reduction in $L_{2\pi}$ can be achieved by setting G/λ_0 to the optimum value. For example, an increase of nearly 30 percent in $\Delta\phi$ and a decrease of nearly 25 percent in $L_{2\pi}$ are obtained in the case of T/λ_0 equal to 0.051.

Figs. 7 and 8 show the frequency characteristics of $\Delta\phi$ and $L_{2\pi}$ for several values of G/λ_0. These curves show that improvements in $\Delta\phi$ and $L_{2\pi}$ are achieved by a reduction of G/λ_0 as long as G/λ_0 is not extremely small.

The RF magnetic field distributions have been computed for various values of G/λ_0, and the results are shown in Figs. 9(a) and (b) for positive and negative circular polarization, respectively. In the conventional configuration ($G=B$), there exists only a small component of circular polarization within the ferrite because the

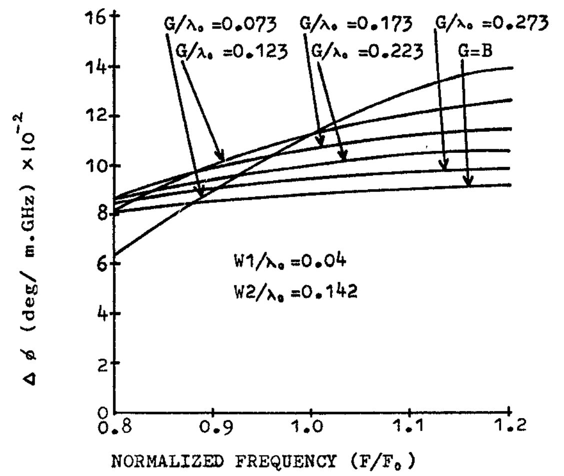

Fig. 7. Differential phase shift ($\Delta\phi$) versus frequency (F/F_0) for several grooved-waveguide heights (G/λ_0).

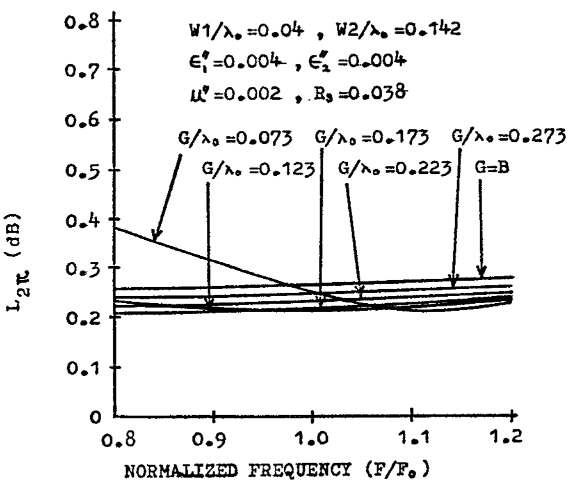

Fig. 8. Loss ($L_{2\pi}$) versus frequency (F/F_0) for several grooved-waveguide heights (G/λ_0).

intensity of the X component (H_x) of the RF magnetic field is larger than that of the Y component (H_y). However, in order to increase $\Delta\phi$, it is desirable to excite the largest possible component of circular polarization. The grooved waveguide achieves this desired enhancement. As shown in Fig. 9, it is possible to generate a larger Y component, and hence a larger component of circular polarization by the appropriate reduction of G/λ_0. It must be noted, however, that the performance becomes poor when G/λ_0 is reduced beyond the optimum value.

The maximum intensity of the RF magnetic field in the ferrite, which occurs for the conventional design at the ferrite-dielectric interface, determines the peak handling power levels of the phase shifter. By decreasing G/λ_0 to the optimum value, the peak handling power level can be increased because the maximum intensity is reduced, as can be seen in Fig. 9.

For example, it will be increased about 10 percent in the handling level of peak power by the reduction of G/λ_0 from 0.323 to 0.123. By the way, the arcing problem is not taken into consideration in the estimation of the peak-power handling ability.

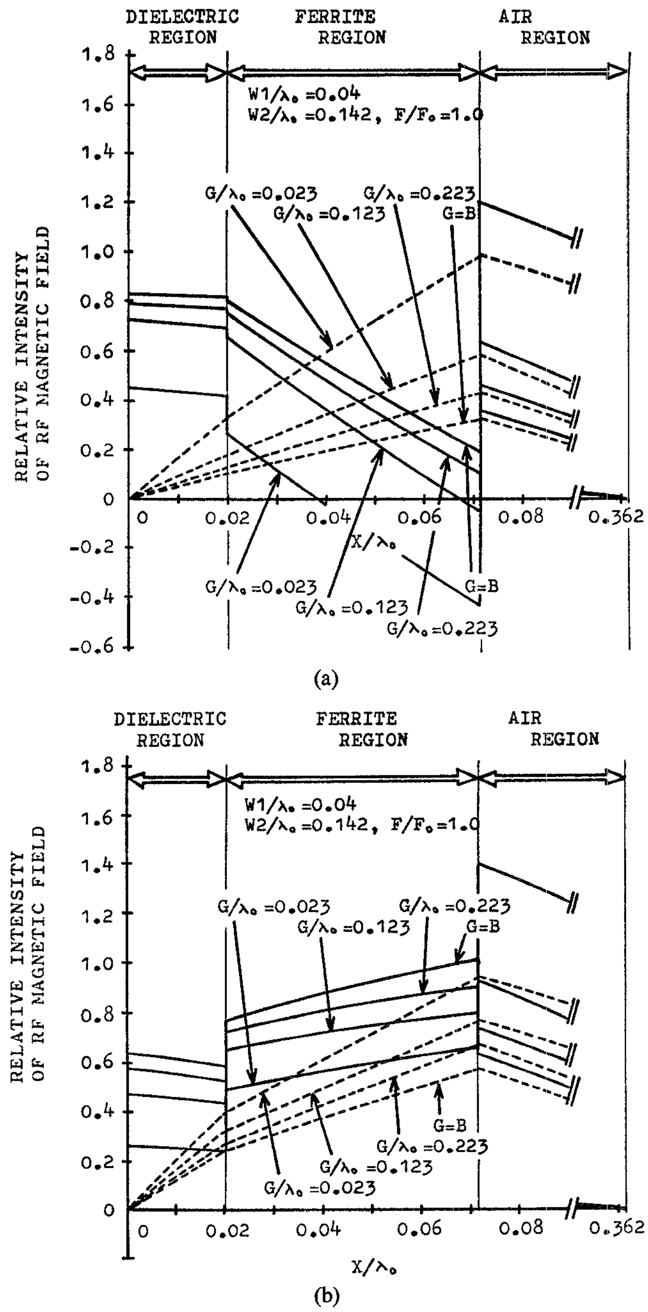

Fig. 9. (a) Relative intensity of RF magnetic field distribution for several grooved waveguide height (G/λ_0) in the case of positive circular polarization. (——— H_x^+,------ H_y^+). (b) Relative intensity of RF magnetic field distribution for several grooved waveguide height (G/λ_0) in the case of negative circular polarization. (——— H_x^-,------ H_y^-).

In this new configuration, it is possible to achieve lower thermal resistance between the ferrite and the waveguide and, therefore, to handle higher average power than in the conventional waveguide design. It is easy to increase the handling level of average power to double by reducing G/λ_0 because the thermal resistance is in inverse proportion to the contact area between the ferrite and the waveguide with the assumption of the ideal heat sink.

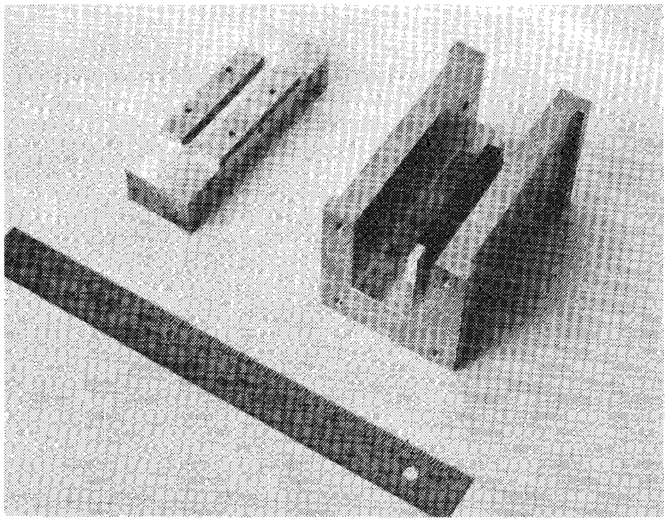

Fig. 10. X-band phase shifter for test.

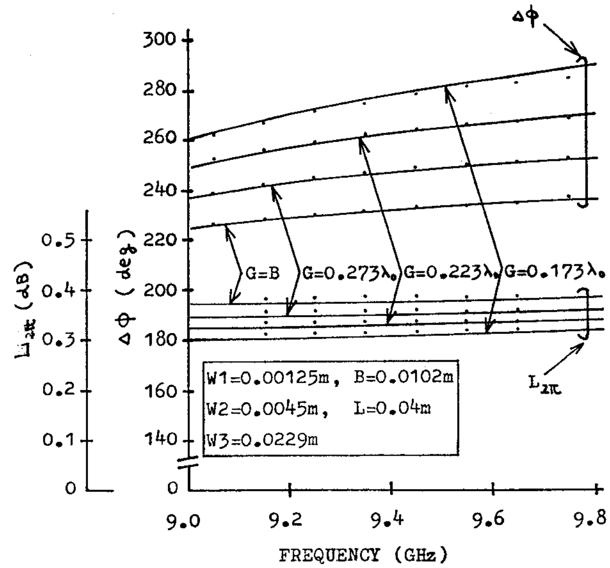

Fig. 11. Frequency characteristics of differential phase shift ($\Delta\phi$) and loss ($L_{2\pi}$).

V. Experimental Results

An X-band phase shifter is shown in Fig. 10.

In Fig. 11, the dots show the experimental values over the frequency range from 9.0 to 9.8 GHz, and the solid lines show the compensated theoretical results which were calculated by using (1) and (2) and by taking into consideration the active [7] dimension of the ferrite. A good agreement between theoretical and experimental values has been obtained.

These results indicate that the figure of merit of the grooved-waveguide phase-shifter configuration are about 20 percent or more above that of the conventional waveguide design.

VI. Conclusion

Some remarkable results of the proposed phase shifter have been reported. It has been shown theoretically and experimentally that at X band the figure of merit can be improved by more than 20 percent in comparison with the conventional one by the adoption of the grooved waveguide with the optimum dimensions.

Moreover, theoretical results indicate that the peak- and average- power handling ability of this new configuration should be enhanced by the more favorable RF magnetic field distribution and the improved thermal contact between the ferrite and the waveguide walls.

References

[1] W. J. Ince, "Recent advances in diode and ferrite phaser technology for phased-array radars," *Microwave J.*, pp. 36–46, Sept. 1972.

[2] W. J. Ince and E. Stern, "Nonreciprocal remanence phase shifters in rectangular waveguide," *IEEE Trans. Microwave Theory Tech.*, vol. MTT-15, pp. 87–95, Feb. 1967.

[3] W. P. Clark, "A technique for improving the figure-of-merit of a twin-slab nonreciprocal ferrite phase shifter," *IEEE Trans. Microwave Theory Tech.*, vol. MTT-16, pp. 974–975, Nov. 1968.

[4] G. P. Rodrigue, J. L. Allen, L. J. Lavedan, and D. R. Taft, "Operating dynamics and performance limitations of ferrite digital phase shifters," *IEEE Trans. Microwave Theory Tech.*, vol. MTT-15, pp. 709–713, Dec. 1967.

[5] L. R. Whicker and R. R. Jones, "Design considerations for digital latching ferrite phase shifters," *Microwaves*, Nov. 1966.

[6] A. Mizobuchi and H. Kurebayashi, "New configurations of the nonreciprocal remanence ferrite phase shifter," 1978 *IEEE Microwave Theory Tech. Symp. Digest*, June 1978.

[7] G. N. Trandoulas, D. H. Temme, and F. G. Willwerth, "Longitudinal section mode analysis of dielectrically loaded rectangular waveguides with application to phase shifter design," *IEEE Trans. Microwave Theory Tech.*, vol. MTT-18, pp. 85–95, Feb. 1970.